Supplementary Information

Three-dimensional graphene-wrapped PANI nanofiber composite as electrode material for supercapacitor

Jiande Wang[a,b,†], Haiyang Xian[a,†], Tongjiang Peng[a,*], Hongjuan Sun[a], Fengxian Zheng[c]

[a] Institute of Mineral Materials & Application, Southwest University of Science and Technology, Mianyang 621010, P.R. China.

[b] School of Material Science and Engineering, Southwest University of Science and Technology, Mianyang 621010, P.R. China.

[c] Wenshang NO.1 Experimental Middle School, Jining 272500, P.R. China.

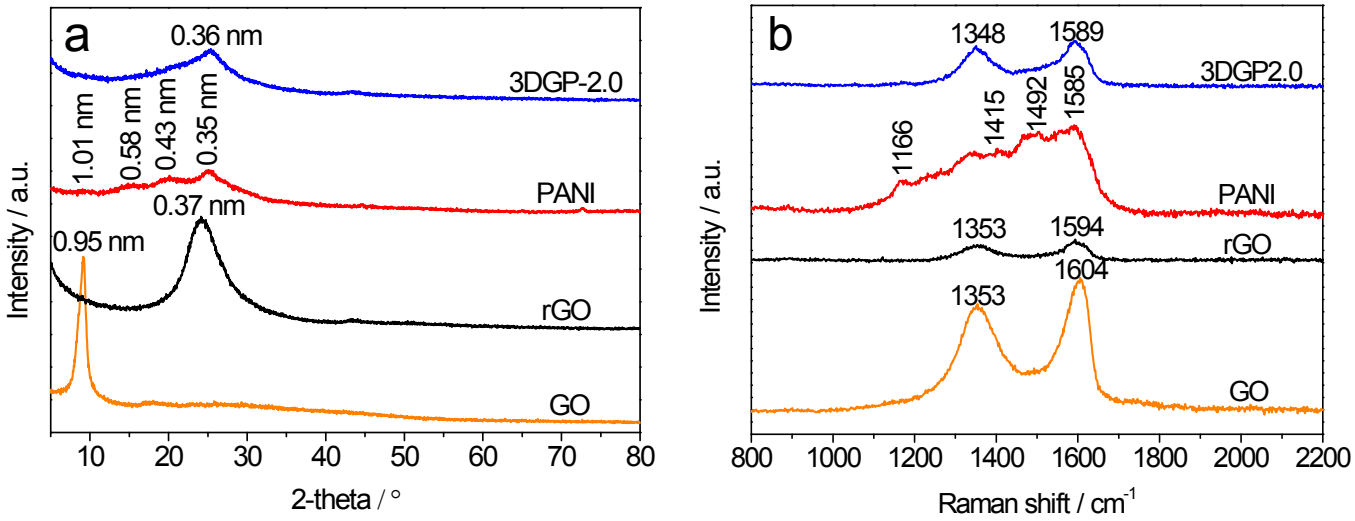

Fig.S1 XRD patterns (a) and Raman spectra (b) of GO, rGO, PANI and 3DGP-2.0.

Fig. S1a shows the XRD patterns of GO, rGO, PANI and 3DGP. It can be seen that the interlayer spacing of rGO (0.37 nm) is much smaller than that of GO (0.95 nm) because most of the oxygenic groups peaks, which can be assigned to the characteristic peak of PANI[1], is observed in the XRD pattern of PANI. Compared with rGO and PANI, the XRD pattern of the 3DGP exhibits one peak similar to that of rGO, but the peaks of PANI are not found, indicating that the PANI in the composite exhibits worse crystallinity than that of pure PANI because of the existence of rGO.

Fig. S1b shows the Raman spectra of GO, rGO, PANI and 3DGP. The spectra of GO and rGO show Raman-active E_{2g} mode at 1600 cm^{-1} ± (G-band), characteristic of the graphitic sheets, whereas a broad D-band centred at 1353 cm^{-1}, which is attributed to the presence of edges and defects within the graphitic sheets[2, 3]. It can be seen that the Raman intensity of rGO is much lower than that of GO and the G-band shift from 1604 to 1594 cm^{-1}. That's because the sp^3 carbon, which is formed during the oxidation process, recovers to sp^2 carbon[4]. The Raman spectrum of PANI shows the typical bands of the polymer. Representative peaks of PANI are also found at 1166, 1415, 1492 and 1585 cm^{-1}, corresponding to C-H bending of the quinoid benzenoid ring, C-C stretching vibration of quinoid rings, C-N stretching band of quinoid rings and C-C stretching vibration of benzenoid[5], respectively. However, the Raman spectrum of 3DGP is different with that of others. One thing is that the Raman intensity of 3DGP is higher than that of rGO which may due to PANI in the structure. The other is the C=C stretching band at 1594 cm^{-1} in rGO red shifts to 1589 cm^{-1} in 3DGP.The results suggest that the benzenoid unit concentration is increased in 3DGP, which gives evidence that a π-π interaction occurs between the quinoid ring of PANI and graphene which can influence the electronic transport properties of the 3DGP.

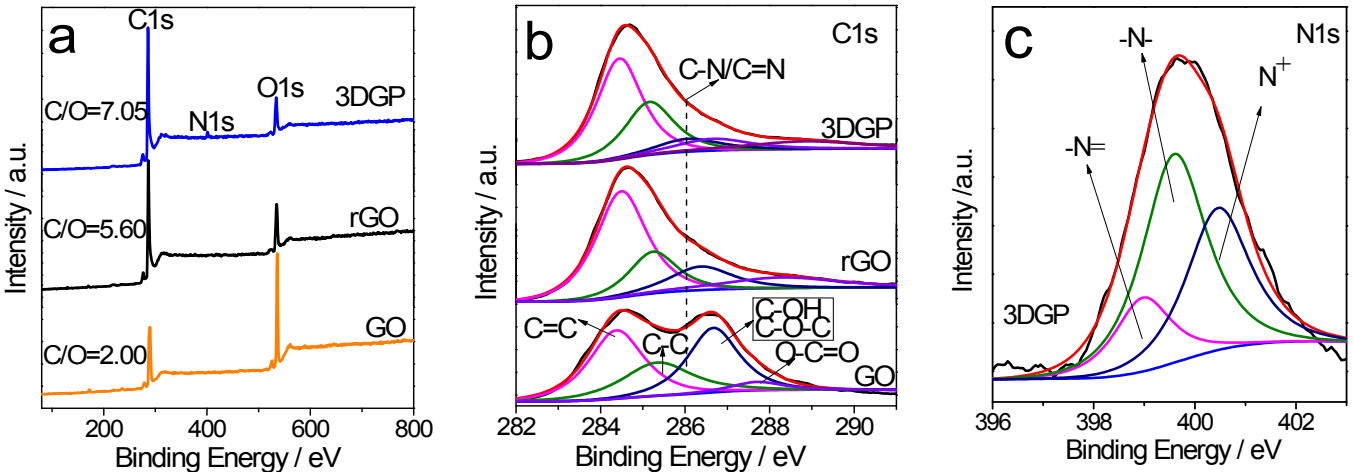

Fig. S2 XPS survey spectra (a), C1s spectra of GO, rGO, 3DGP-2.0 (b) and N1s spectrum of 3DGP-2.0 (c).

Fig. S2 shows XPS spectra of GO, rGO and 3DGP. In Fig. 4a, both spectra of GO and rGO exhibit two main peaks at ~533 and ~285 eV, corresponding to O 1s and C 1s spectra, respectively. Another peak at ~400 eV, corresponding to N 1s spectrum[6], can also be identified in the survey spectrum of 3DGP. The results of C/O ratio calculated from the area of the peaks are also presented in Fig. 4a. It can be seen that the C/O ratio increases from 2.00 in GO to 5.60 in rGO after the hydrothermal process. The C/O ratio of 3DGP increase to 7.05 due to the addition of PANI in the structure. Fig. 4b shows the C 1s spectra of GO, rGO and 3DGP. It can be seen that the C 1s peaks of GO and rGO consists of four peaks arising from C=C (~284.50 eV), C-C (~285.20 eV), C-O/C-O-C (hydroxyl or epoxy, ~286.50 eV) and C=O (carbonyl, ~288.65 eV) groups[7]. A peak at ~286.00 eV arising from C-N/C=N can also be identified in the C 1s spectrum of 3DGP[8], suggesting that PANI is presented in the composite. The N 1s peak of 3DGP is shown in Fig. 4c. The peak is broad indicating the existence of different bond structures in 3DGP. According to the previous works[9], they can be identified as neutral andimine-like structure nitrogen atoms (=N-), neutral and amine-like nitrogen atoms (-NH-) and cationic nitrogen atoms (N^+).

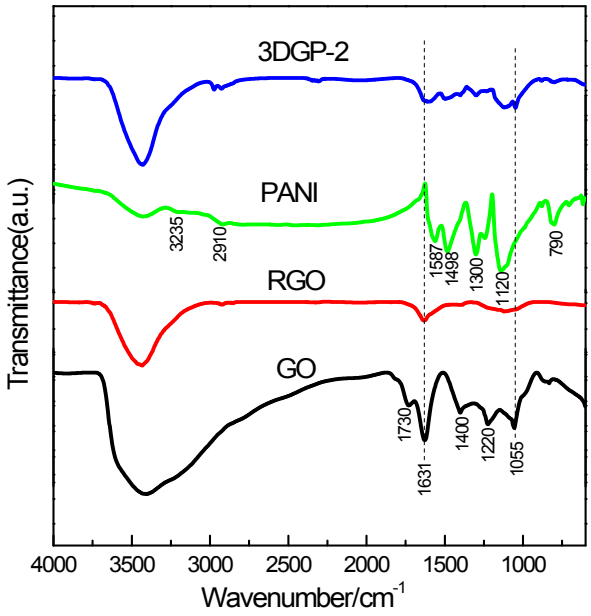

Fig. S3 FT-IR spectra of GO, rGO, PANI and 3DGP-2.0.

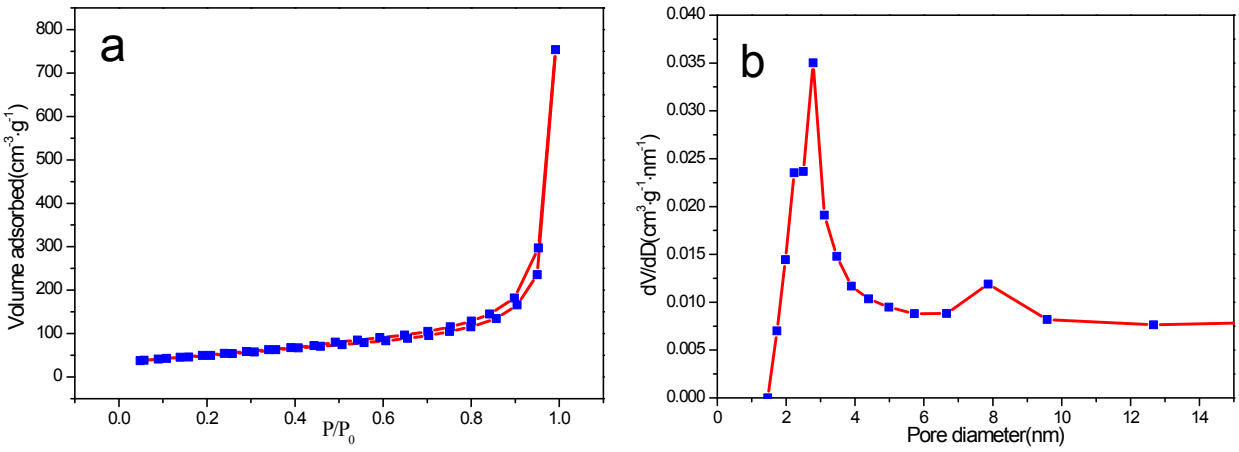

Fig. S4 (a) N_2 adsorption–desorption isotherms of and (b) pore size distributions from adsorption branches for 3DGP-2.0 calculated by BJH method.

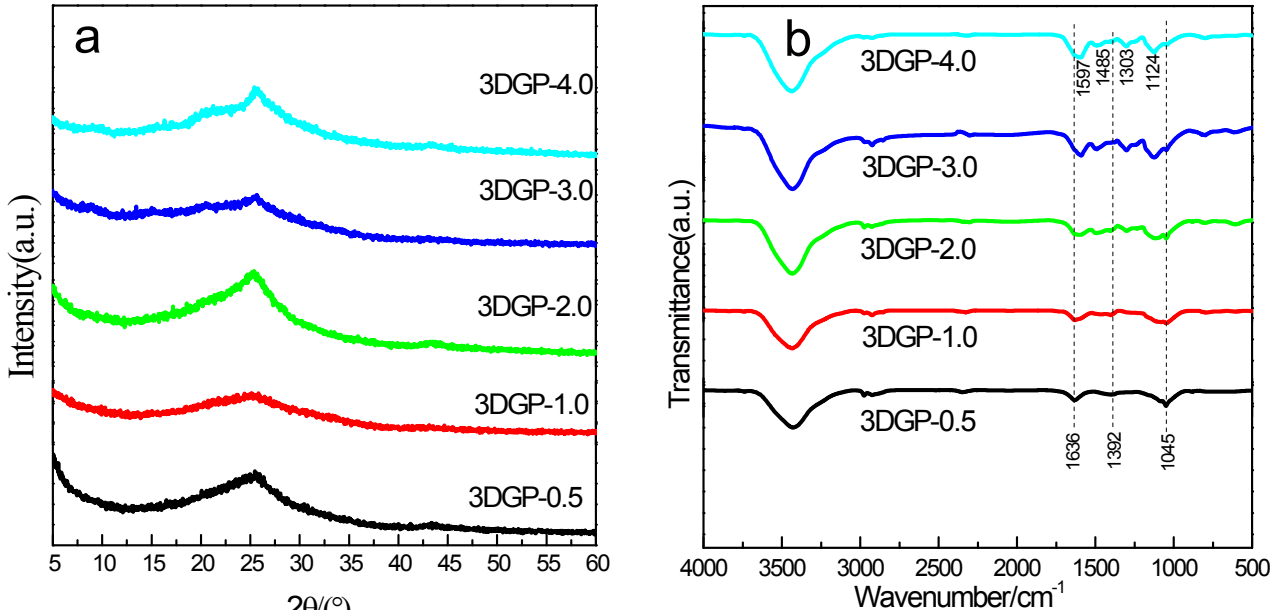

Fig. S5 XRD patterns (a) and FT-IR spectra (b) of 3DGP-*n*.

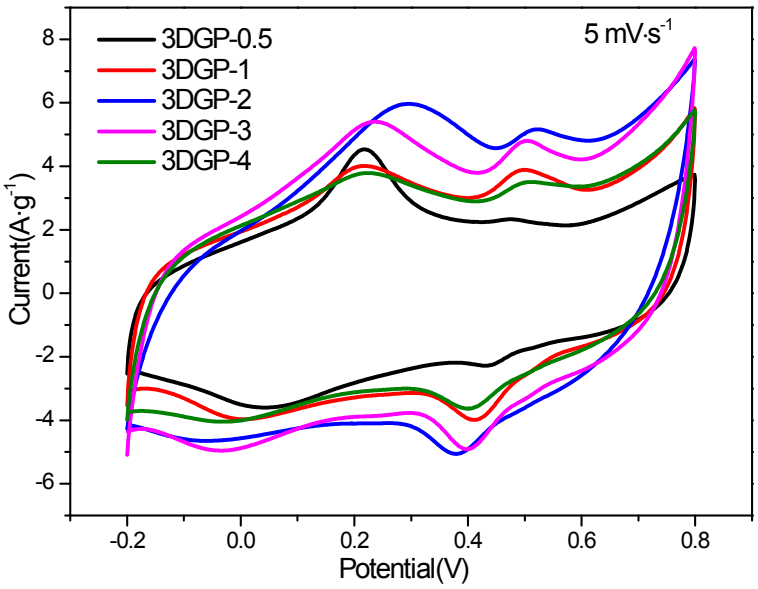

Fig. S6 CV curves at 5 mV s^{-1} of 3DGP-*n*.

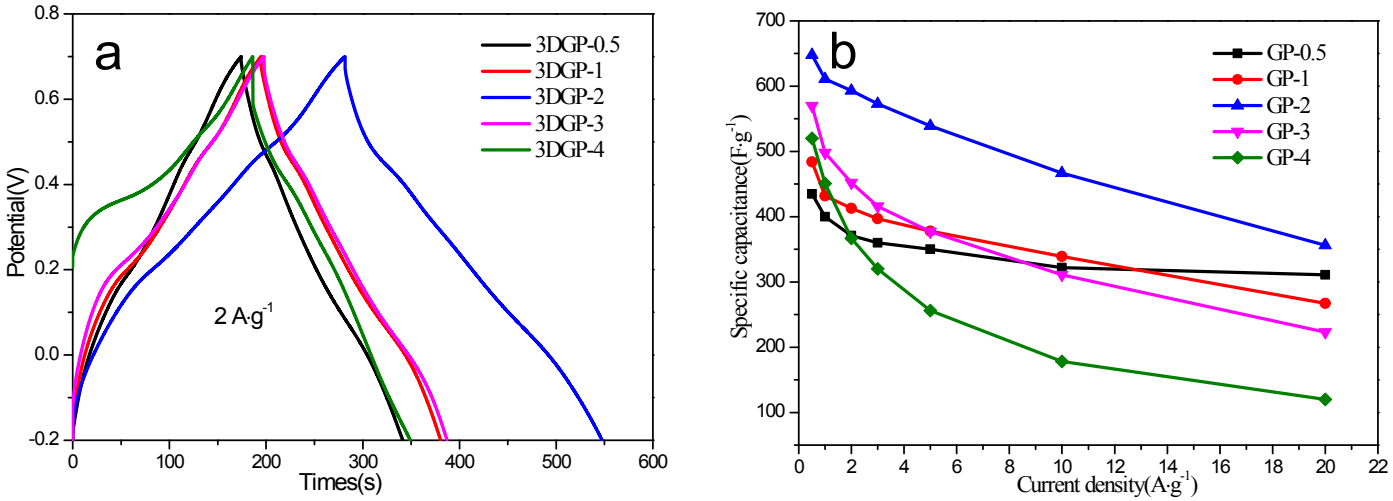

Fig. S7 (a) GCD curves at 2 A g^{-1} and (b) specific capacities at different current densities of 3DGP-*n*.

References

1. H. L. Yu, T. S. Wang, B. Wen, M. M. Lu, Z. Xu, C. L. Zhu, Y. J. Chen, X. Y. Xue, C. W. Sun and M. S. Cao, *Journal Of Materials Chemistry*, 2012, **22**, 21679-21685.
2. F. Tuinstra and J. L. Koenig, *The Journal of Chemical Physics*, 1970, **53**, 1126.
3. M. Pimenta, G. Dresselhaus, M. S. Dresselhaus, L. Cancado, A. Jorio and R. Saito, *Physical Chemistry Chemical Physics*, 2007, **9**, 1276-1290.
4. J. W. An, J. H. Liu, Y. C. Zhou, H. F. Zhao, Y. X. Ma, M. L. Li, M. Yu and S. M. Li, *J Phys Chem C*, 2012, **116**, 19699-19708.
5. Y. Z. Liao, C. Zhang, X. Wang, X. G. Li, S. J. Ippolito, K. Kalantar-Zadeh and R. B. Kaner, *J Phys Chem C*, 2011, **115**, 16187-16192.
6. H. L. Wang, Q. L. Hao, X. J. Yang, L. D. Lu and X. Wang, *Nanoscale*, 2010, **2**, 2164-2170.
7. C. Z. Zhu, S. J. Guo, Y. X. Fang and S. J. Dong, *Acs Nano*, 2010, **4**, 2429-2437.
8. S. Golczak, A. Kanciurzewska, M. Fahlman, K. Langer and J. J. Langer, *Solid State Ionics*, 2008, **179**, 2234-2239.
9. V. R. Gedela and V. V. S. S. Srikanth, *Synthetic Metals*, 2014, **193**, 71-76.